Reduced Gyral Window and Corpus Callosum Size in Autism: Possible Macroscopic Correlates of a Minicolumnopathy

Manuel F. Casanova, et al.

Journal of Autism Developmental Disorders, 2009

NeuroSpectrum Insights, Inc.
info@neurospectruminsights.com
www.neurospectruminsights.com

J Autism Dev Disord (2009) 39:751–764
DOI 10.1007/s10803-008-0681-4

ORIGINAL PAPER

Reduced Gyral Window and Corpus Callosum Size in Autism: Possible Macroscopic Correlates of a Minicolumnopathy

Manuel F. Casanova · Ayman El-Baz · Meghan Mott · Glenn Mannheim · Hossam Hassan · Rachid Fahmi · Jay Giedd · Judith M. Rumsey · Andrew E. Switala · Aly Farag

Published online: 16 January 2009

Abstract Minicolumnar changes that generalize throughout a significant portion of the cortex have macroscopic structural correlates that may be visualized with modern structural neuroimaging techniques. In magnetic resonance images (MRIs) of fourteen autistic patients and 28 controls, the present study found macroscopic morphological correlates to recent neuropathological findings suggesting a minicolumnopathy in autism. Autistic patients manifested a significant reduction in the aperture for afferent/efferent cortical connections, i.e., gyral window. Furthermore, the size of the gyral window directly correlated to the size of the corpus callosum. A reduced gyral window constrains the possible size of projection fibers and biases connectivity towards shorter corticocortical fibers at the expense of longer association/commisural fibers. The findings may help explain abnormalities in motor skill development, differences in postnatal brain growth, and the regression of acquired functions observed in some autistic patients.

Keywords Autistic disorder · Corpus callosum · Magnetic resonance imaging · Telencephalon

Introduction

Infantile autism is a behaviorally defined condition. Afflicted individuals exhibit deviations in the normal development of social relationships, language/communication skills, and

Dr. Mannheim is affiliated with the Food and Drug Administration; however, this article was written in his private capacity. No official support or endorsement by the Food and Drug Administration is intended or should be inferred.

This work was written as part of Judith Rumsey's and Jay Giedd's official duties as Government employees. The views expressed in this article do not necessarily represent the views of the National Institute of Mental Health, the National Institutes of Health, the Department of Health and Human Services, or the United States Government.

M. F. Casanova (✉) · M. Mott · A. E. Switala
Department of Psychiatry, University of Louisville,
500 South Preston St. Bldg. 55A Ste 210,
Louisville, KY 40292, USA
e-mail: manuel.casanova@louisville.edu;
m0casa02@gwise.louisville.edu

A. El-Baz
Department of Bioengineering, University of Louisville,
Louisville, KY, USA

G. Mannheim
Division of Psychiatry Products, Food and Drug Administration,
Silver Spring, MD, USA

H. Hassan · R. Fahmi · A. Farag
Department of Electrical and Computer Engineering,
University of Louisville, Louisville, KY, USA

J. Giedd
Child Psychiatry Branch, National Institute of Mental Health,
Bethesda, MD, USA

J. M. Rumsey
Neurodevelopmental Disorders Branch, National Institute
of Mental Health, Bethesda, MD, USA

Present Address:
J. M. Rumsey
Division of Adult Translational Research, National Institute
of Mental Health, Bethesda, MD, USA

repetitive patterns of behavior. It is a disorder of wide clinical spectrum, most often idiopathic in nature, but also shown to be associated with a group of etiologically heterogeneous disorders, such as fragile × syndrome, tuberous sclerosis, and congenital rubella. In recent years interest in the neuropathology of autism has been spurred by the studies of Bauman and Kemper (1985, 1988, 1994) and their efforts at tissue collection. Researchers now accept that brains of individuals with autism are larger than normal in early life due to accelerated brain growth (Courchesne et al. 2001, 2003). Differences in mean brain size between the two groups have diminished by adolescence, largely as a result of increased relative growth in nonautistic individuals (Courchesne et al. 2001; Aylward et al. 2002; Sparks et al. 2002). In some case series, brain weights/volumes are larger or heavier, and in a fraction of cases brain mass exceeds 1,800 g, consistent with megalencephaly (Friede 1989; Courchesne et al. 1999). As expected, the hyperplasia of brain tissue affects a major portion of the cerebrum (Piven et al. 1996). The data suggest that the neuropathological underpinning of autism affects multiple systems or involves widespread areas of the brain, rather than discrete anatomical structures (Bailey et al. 1996).

Our group and others have recently described abnormalities in the minicolumnar arrangement of neurons within the neocortex of individuals with autism (Buxhoeveden et al. 2006; Casanova et al. 2006b, c). Minicolumns in the brains of autistic patients were narrower and more numerous per linear length of tissue section examined as compared to controls. Since the minicolumn re-iterates itself millions of times throughout the brain, variations in the total number and width of minicolumns can result in macroscopic changes of the brain's surface area and/or gyrification (Armstrong et al. 1991). In effect, Rakic (1995) has proposed that the combination of brain growth (encephalization) and the relative preservation in cortical thickness across mammalian species stems from an increase in the total number of minicolumns. Support for this hypothesis is derived from studies that have either increased (Chenn and Walsh 2003; Tarui et al. 2005) or decreased (Kuida et al. 1996; Haydar et al. 1999) the number of proliferative units within the ventricular zone during brain development. An increase in the number of minicolumns may lead to an increase in brain size and thus provides a putative explanation to the macroencephaly of autism.

The proper integration of supernumerary minicolumns, both into corresponding segregates and their lateralized hemispheric homologues, requires their interconnectivity via association and commissural fibers (Hofman 2001). According to Hofman (2001), "neocorticalization in primates is mainly due to the progressive expansion of the axonal mass, rather than an increase in the number of cortical neurons." Evolution has therefore required that bigger brains decrease their gray/white matter ratio (i.e., have a comparative increase in their white matter) while leaving intact the size of structures defined by projection fibers to extratelencephalic sites. Recent magnetic resonance imaging (MRI) studies noting an increase in brain size, decreased gray/white matter ratio, and altered arrangement of white matter fibers in autism may therefore be explained within the context of minicolumnar pathology (Goldberg et al. 1999; Courchesne et al. 2001; Herbert 2005; Keller et al. 2007).

In this study, a series of autistic patients were studied for morphometric parameters related to minicolumnar pathology: cortical thickness, gray/white matter ratio, corpus callosum size and shape, cortical folding as measured by the gyrification index (GI), and depth of gyral white matter (a proxy measurement for gyral window). The gyral window refers to the space or aperture of passage for all projections coming in or out of the cortex, i.e., cortical afferent/efferent fibers (Prothero and Sundsten 1984). It is important to note that the human GI averages 2.56 (SD 0.03) which is the amount expected for a nonhuman anthropoid (ape and monkey as distinguished from prosimians) if we expanded its brain to human dimensions. That is, the human values are predictable given the association between GI and brain weight/volume in nonhuman anthropoids. It is therefore not surprising that absolute brain size has, by tradition, been considered an important determinant for cortical folding (Brodmann 1913; Zilles et al. 1989). Conclusions regarding gyrification should therefore originate from comparison series matched for brain size, or employing suitable correction factors. In the present study the comparison cases were matched for age, gender, handedness, and cerebral volume.

Methods

Patient Sample

Fourteen male subjects between 8 and 38 years of age (mean 22.5 year; SD 9.9 year) were recruited from across the United States (Table 1). DSM-III-R and the Autism Diagnostic Interview (ADI) criteria were used to define autism, autistic disorders, and pervasive developmental delay. ICD-10 and the proposed criteria of Szatmari et al. (1989) were used to define Asperger's syndrome. WAIS-R IQs ranged from 65 to 107 (mean 82; SD 5.2). None had significant medical problems by history and physical examination with the exception of one patient who had a history of a single complex partial seizure 11 years prior to MRI acquisition, for which he was maintained on phenytoin without any recurrence. No others were on medication at the time of the study. There was no diagnosed etiology to their developmental delay.

Table 1 Clinical data for patients with autism spectrum disorder

	Age	Primary diagnosis	Secondary diagnoses	Medications
1.	8.04	Autistic disorder	OCD	Chlorimipramine; desipramine
2.	8.42	Autistic disorder	OCD	Chlorimipramine
3.	11.74	Autistic disorder	OCD	Chlorimipramine
4.	14.25	Autistic disorder	OCD	Chlorimipramine
5.	19.54	Autistic disorder		
6.	19.55	Autistic disorder		Lorazepam
7.	20.17	Autistic disorder		
8.	20.91	Autistic disorder		
9.	25.64	Autistic disorder		
10.	28.02	Autistic disorder		
11.	32.71	Autistic disorder	Asthma; hypercholesterolemia	Buspirone; doxycycline
12.	33.57	Autistic disorder	Epilepsy	Phenytoin
13.	34.85	Autistic disorder		
14.	38.17	Autistic disorder	Bipolar disorder	Benztropine; haloperidol; lithium

Age is the patient's age in years at the time of MRI acquisition. All patients were male. *OCD* obsessive-compulsive disorder

Screening of autistic patients comprised independent observations of the subjects' behavior, review of past medical/pediatric/psychiatric records, and interviews with parents regarding perinatal, medical, and developmental histories. Standard laboratory tests were performed to exclude common metabolic problems that might impact on the subject's cognition. In addition, chromosomal analysis (including Fragile × evaluations) was obtained on all patients with autism spectrum disorders. Informed consent and assent were obtained from the parent(s) and patient, respectively, prior to the start of the study.

Twenty-eight male, non-autistic individuals, matched 2:1 with patients for age (mean 22.6 year; SD 9.9 year) and handedness, were recruited for comparison. Comparison subjects were without significant medical and psychiatric problems in themselves or in first-degree relatives. They had normal physical and neurological examinations and were on no medications.

Magnetic Resonance Images

Subjects were scanned on a 1.5 T GE MRI using IR and FLASH volume sequences. Subjects' placement was standardized. A full scan was composed of a 3D acquisition of 124 axial or coronal slices. Spacing between slices was 1.5 mm in the axial volumes or 2.0 mm in the coronal volumes. In either case, pixel dimensions in the slice plane were 0.9375 mm × 0.9375 mm. Some measurements, like the brain outlines for computing gyrification index, were made using slices in a particular orientation (coronal in the case of GI), regardless of the MRI acquisition sequence. For these purposes, the scans were re-sliced as needed, interpolating values of resampled voxels lying between voxels in the original volume.

Image Processing

All images were preprocessed to reduce scanner noise (Fig. 1). This minimized the gray level difference between

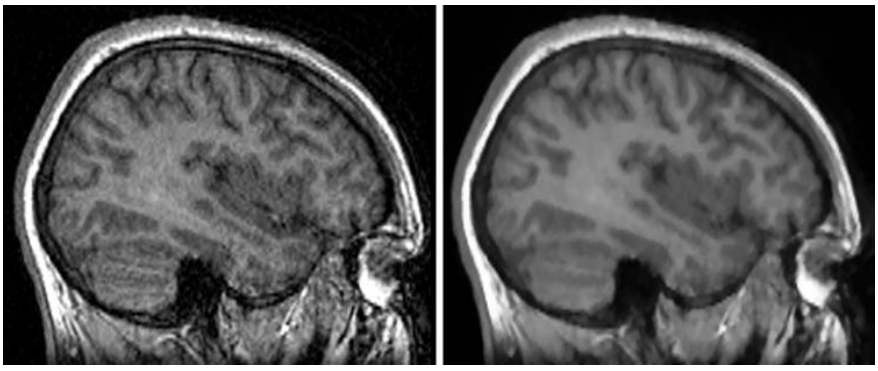

Fig. 1 An MRI scan re-sliced in the sagittal plane, before (*left*) and after (*right*) noise reduction

each voxel and its neighbors. To this end we used a Gibbs-Markov Random Field model for each MRI data set. Gradient descent was used to find the optimum gray level g_{opt} at each location $k = (x_k, y_k, z_k)$ that minimizes the Gibbs energy (Bouman and Sauer 1993):

$$g_{opt}(k) = \arg\min_{g} \left(|g(k) - g|^{\tau} + \sigma^{\tau} \lambda^{\rho} \sum_{r \in N(k)} b |g(r) - g|^{\rho} \right),$$

where b, λ, ρ, σ, and τ are constants and $N(k)$ is the 26-neighborhood of voxel k, i.e.

$$\{(x, y, z) : \max\{|x - x_k|, |y - y_k|, |z - z_k|\} = 1\}.$$

We used a priori learned visual appearance models of cerebral white matter to control the evolution of the deformable model in the segmentation process. Control points on the deformable surface ∂V are introduced, removed, or shifted to minimize the boundary energy (Kass et al. 1988):

$$E = \int_{\partial V} (\xi_{int} + \xi_{ext}) \cdot ds,$$

where ξ_{int} and ξ_{ext} are internal and external forces, respectively. The functional form of ξ_{ext} was based on two new probability models that roughly describe the prior and current visual appearance, as described in recent publications (El-Baz et al. 2006, 2007a).

Morphometric Parameters

Each quantity was the product of either a totally computerized routine or a semi-automatic method where the sample was randomized such that the operator had no knowledge of whether a case was a patient or control during the measurement procedure.

Gyral Window

To quantify the gyral window (w), we extracted the cerebral white matter in all cortical gyri from the segmented cerebral white matter. The approach that we used is based on calculating the distance map inside the 3D segmented cerebral white matter using a fast marching level set method (Adalsteinsson and Sethian 1995). The distance map at any point inside the segmented object is defined as the minimum Euclidean distance from the boundary (Fig. 2). We used a Gaussian mixture model (El-Baz et al. 2006) to estimate the marginal density for distances that belong to cerebral white matter gyrifications (class 1) and distances that belong to the other cerebral white matter tissues (class 2). Using the marginal density, we extracted the cerebral white matter within gyri by estimating the best threshold—gyral window w—that discriminated between the distances from cerebral white matter gyrifications and distances to other cerebral white matter tissues (El-Baz et al. 2007a, b; Fahmi et al. 2007).

Corpus Callosum Displacement

The first step in calculating the displacement (CC) of the corpus callosum was to segment the structure automatically from MRI images based on learning its prior appearance model. For each group (autistic and normal), we randomly picked four CC data sets, one of which was chosen as reference and the remaining ones are registered to it using our deformable registration method (Fahmi et al. 2006). During these registration steps, a deformation field was

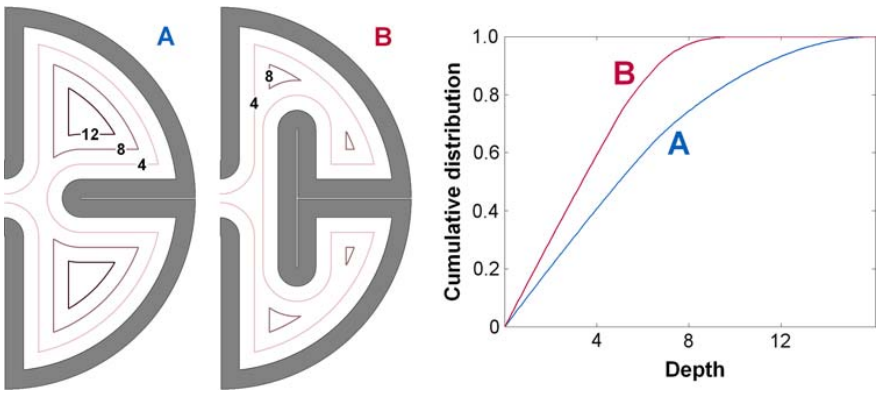

Fig. 2 *Left*: Phantom cerebral hemispheres with lesser (**a**) and greater (**b**) gyrification. Contours inside the white matter indicate those points at a distance of 4, 8, or 12 arbitrary units from the exterior white matter boundary. *Right*: The cumulative distribution of white matter $F(d)$ is the proportion of white matter a distance d or less from the boundary. With greater gyrification, boundary surface area increases without a concomitant increase in white matter volume. Proportionally more white matter is found nearer the boundary. This is reflected in a steeper cumulative distribution function

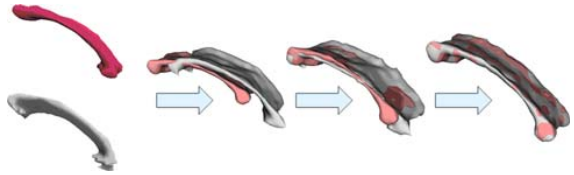

Fig. 3 Computation of corpus callosum displacement. Segmented corpora callosa (*left*) from two different individuals are shown in the same coordinate system prior to alignment (*second panel*). The two are registered as closely as possible using only translation, rotation, and uniform scaling (*third panel*). Then one is deformed to match the shape of the other precisely (*right*). Displacement CC is the distance by which points on one corpus callosum surface are moved toward the other surface by the deformation step

generated for each alignment with the three reference data sets. These deformation fields were then averaged, and a cumulative distribution function computed to represent the changes of the magnitudes of each one of the averaged deformation fields (Fig. 3). These distributions served for classification purposes.

Cortical Thickness

Cortical thickness (t) was computed stereologically. A set of randomly oriented test lines with total length L is superimposed on the image, and the operator counts the number of intersections P of these lines with the gray matter-CSF boundary. The stereological S_V, the surface area per unit volume, is then $2P/L$. The volume fraction V_V is the area of the gray matter divided by the area of the region of interest. Cortical thickness can be expressed as V_V/S_V, which is unbiased provided the cortex intersects the plane of section orthogonally. To minimize bias, t was measured using the five axial slices nearest the mid-axial plane.

Medulla Oblongata Cross-section

The cross-sectional area of the medulla oblongata (MO) was found by manually outlining the structure in the axial plane. The plane of section was chosen to be midway between the base of the pons and the beginning of the spinal cord.

Gray/White Matter Ratio

The gray matter/white matter ratio ($G{:}W$) was found by first selecting two thresholds to segment the brain into gray matter, white matter, and CSF. Then the volume was resampled in sagittal slices spaced 7.5 mm apart. In each slice containing brain matter, the operator drew a rough outline around the cortical gray matter and subcortical white matter, including the corpus callosum. Subcortical gray matter was excluded. The interior of the outline was segmented using the thresholds. At the end of this process the gray/white ratio was the total cross-sectional area of gray matter divided by the total cross-sectional area of white matter.

Gyrification Index

The gyrification index (GI) measurements were made in the coronal plane. Forty slices were randomly selected. In each slice, the operator manually outlined the left cerebral hemisphere, then the right, following the undulations of the gray matter. The convex hull of each outline, i.e., the smallest convex body containing it, was computed automatically. The gyrification index of the section is the ratio of the length of each outline to the perimeter of its convex hull (Fig. 4). The gyrification index has been shown to vary with position along the rostral-caudal axis (Armstrong et al. 1991). Nonparametric regression, or smoothing, was used to find the mean GI as a function of position for the control brains. The raw measurements $g(x_k)$, $1 \leq k \leq 40$, for each control and case of autism were detrended using the smooth curve s and then averaged to obtain the corrected GI:

$$\mathrm{GI} = \frac{1}{40}\sum_{k=1}^{40} \tilde{g}(x_k), \text{ where } \tilde{g}(x) = g(x)\frac{\langle s \rangle}{s(x)}$$

x is relative position along the rostral-caudal axis, and $\langle s \rangle$ is the mean value of $s(x)$.

Armstrong and colleagues (1995) noted that cerebral gyration increases rapidly during development in utero and continues to increase in the postnatal period, reaching a maximum value around 1 year of age. This is followed by a gradual decline until stabilizing at its adult value. The youngest patients in our sample are expected to have a GI appreciably greater than the GI of adult patients. Raw GI measurements were adjusted to remove the effects of normal development:

$$\mathrm{GI}_{\mathrm{adj}} = 1 + (\mathrm{GI} - 1)\frac{f_\infty}{f(t)}.$$

Here, $1 + f(t)$ is the model of GI with respect to time in ontogenetic weeks according to Armstrong et al. (1995), and f_∞ is the horizontal asymptote of f, approximately equal to 1.56.

Corpus Callosum Cross Section

The cross-sectional area of the corpus callosum (CCx) was determined by manually outlining the structure in the sagittal plane. Volumes were resliced sagittally, and measurement was performed in the slice most closely aligned with the longitudinal fissure.

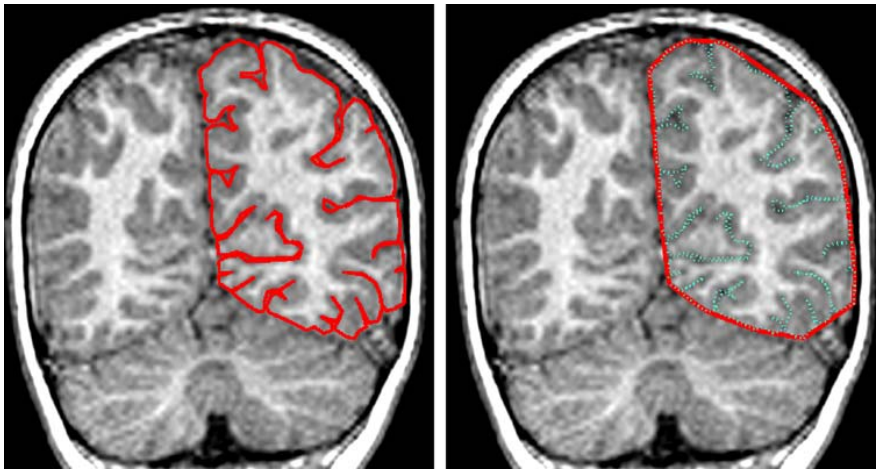

Fig. 4 Measurement of the gyrification index (GI). The outline of the cortical surface of one hemisphere is traced in a coronal section (*left*). The profile's convex hull, the smallest convex set containing the outline, is computed automatically (*right*). Let s be the arc length of the outline, and let p be the perimeter of its convex hull; then $GI = s/p$. Thus, $GI \geq 1$ by definition, and larger values correspond to a greater degree of nonconvexity. Repeating this process in a number of coronal sections along the rostral-caudal axis and again in the other hemisphere provides a mean GI for the brain

Statistics

One scan was excluded due to severe motion artifact, rendering several measurements unobtainable and the remainder questionable. The remaining sample comprised 14 autistic patients and 27 normal comparison cases. Diagnosis was encoded hierarchically in an ANOVA model. The logarithm of patient age was included as a covariate.

The relationship between gyral and interhemispheric communication was analyzed separately using linear regression of gyral window with respect to corpus callosum displacement. Both the slope and intercept were potentially diagnosis dependent, where diagnosis had the same hierarchical encoding as above.

Differences in white matter distribution were further characterized using a classification algorithm based on the Lévy distance between distribution functions,

$$\rho(F,F_t) = \inf\{\delta > 0 : (x)F_t(x-\delta) - \delta \leq F(x) \leq F_t(x+\delta) + \delta\}.$$

When using $\rho(F,F_t)$ for classification, F_t denotes the cumulative distribution function (CDF) of cerebral white matter for the test case, and F is the average CDF of one of the classes (i.e., autistic or normal control). The test case is assigned to the class with the smallest ρ, except that if the Lévy distance to the other class is insignificant for a given confidence level α, the test case is considered ambiguous and not assigned to any class. In judging classifier performance, half the cases, randomly selected, were used to generate class CDFs, and a test case being either mislabeled or ambiguous was considered a classification error.

Table 2 Mean values and pooled standard deviations of morphometric parameters

Parameter	Mean		Standard deviation	
	Normal	Autistic	Normal	Autistic
w (mm)	5.84	2.37	0.22	1.41
CC (mm)	2.92	3.81	1.44	1.81
t (mm)	3.04	3.08	0.19	0.22
G:W	1.56	1.57	0.40	0.21
MO (cm^2)	2.36	2.02	0.35	0.30
GI	1.93	1.95	0.06	0.09
CCx (cm^2)	6.62	5.27	0.99	0.67

w gyral window; *CC* corpus callosum displacement; *t* cortical thickness; *G:W* gray/white matter ratio; *MO* medulla oblongata cross-section; *GI* gyrification index; *CCx* corpus callosum cross section. Some quantities vary significantly with age; mean values were calculated for the median sample age of 22 years

Results

The omnibus tests of dependent variables *w*, CC, *t*, *G:W*, and MO were statistically significant for autism ($F_{5,33} = 369$; $p < 0.0001$) and age ($F_{5,33} = 7.74$; $p = 0.0001$). Significant effects for each measurement individually (Table 2) were as follows.

1. *w*: Autism ($F_{1,37} = 270$; $p < 0.0001$).
2. CC: Autism ($F_{1,37} = 7.90$; $p = 0.0079$).
3. *t*: None.
4. *G:W*: Age ($F_{1,37} = 39.6$; $p < 0.0001$).
5. MO: Autism ($F_{1,37} = 8.17$; $p = 0.007$).

Statistical analysis shows that there is a significant difference between the gyral window of autistic and normal control subjects following the pattern of the full white matter distribution (Fig. 5). The cumulative distribution functions of individual patients cluster tightly around the average CDF for their respective diagnostic categories. This implies that it may be feasible to classify individuals based on white matter distribution. The classifier labels a test case based on the Lévy distance between its white matter CDF and the average CDF of each of the autistic and normal samples, the test case being excluded from the averaging. The classifier was tested for three values of α (Table 3).

The gyral window w was highly correlated with t within diagnostic categories (Fig. 6). The adjusted coefficient of determination of the regression is $R^2 = 0.9966$. There was a significant diagnosis dependence in both the slope ($F_{1,35} = 7.42$; $p = 0.010$) and intercept ($F_{1,35} = 25.0$; $p < 0.0001$) of the regression line. The fitted model is

$$w = 2.81\,\text{mm} - 0.14t$$

for autistic patients and

$$w = 7.25\,\text{mm} - 0.48t$$

Table 3 Diagnostic sensitivity and specificity of the Lévy distance-based classification algorithm

α	85%	90%	95%
Sensitivity	80%	73%	67%
Specificity	96%	96%	89%

The confidence level α is a parameter of the method. The decrease in diagnostic power for higher α corresponds to a greater probability of ambiguous cases being left unclassified

in subjects without autism. Hence, with decreasing gyral window there is concomitant deviation in the corpus callosum, but w does not vary sufficiently with t to attribute changes in w in autism to laterality alone.

F-tests revealed no significant difference in GI_{adj} (Fig. 7) between patients with autistic disorders and normal controls ($F_{1,37} = 0.98$; $p = 0.329$). The cross section CCx differed between autistic subjects and comparison cases ($F_{1,37} = 9.55$; $p = 0.004$). Corpus callosum cross section also increased significantly with age ($F_{1,37} = 9.63$; $p = 0.004$). Interestingly, GI_{adj} does not correlate with w (Spearman $r_s = 0.008$; $p = 0.96$), nor does CCx correlate strongly with CC ($r_s = -0.18$; $p = 0.27$).

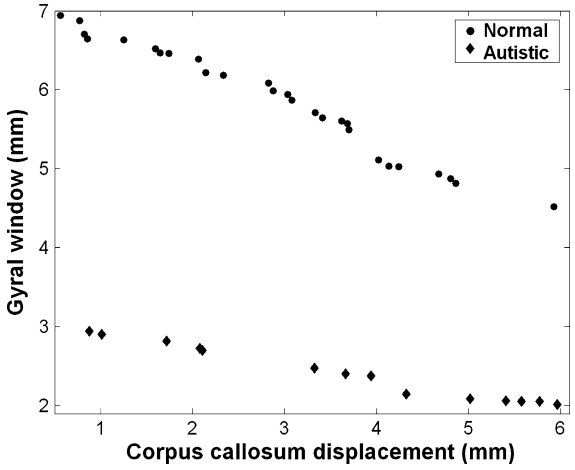

Fig. 6 With increased gyrification (constriction of the gyral window) there is a correlated diminution in the number of long corticocortical connections, reflected in the shape of the corpus callosum

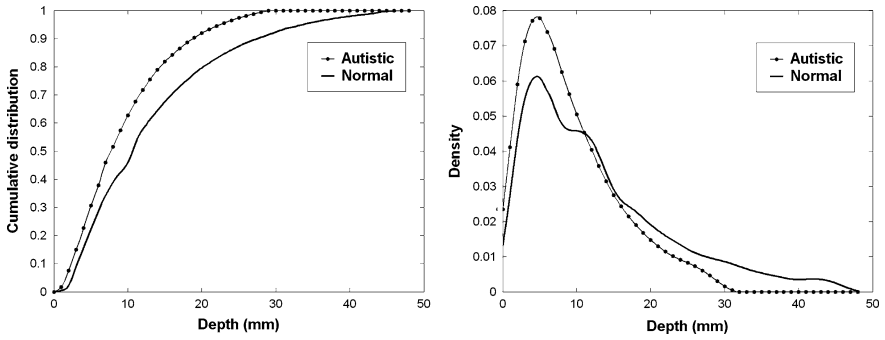

Fig. 5 Visualization of differences in white matter distribution. Narrower gyri (small w) in autism correspond to shallower white matter. *Left*: The cumulative distribution functions (CDFs) of white matter for each of the diagnostic categories show the proportional volume of white matter within a given distance of the white matter surface. These are the pointwise means of the CDFs for all brains within each category. *Right*: Density functions, computed from the CDFs by numerical approximation of their derivatives, provide another view of the same

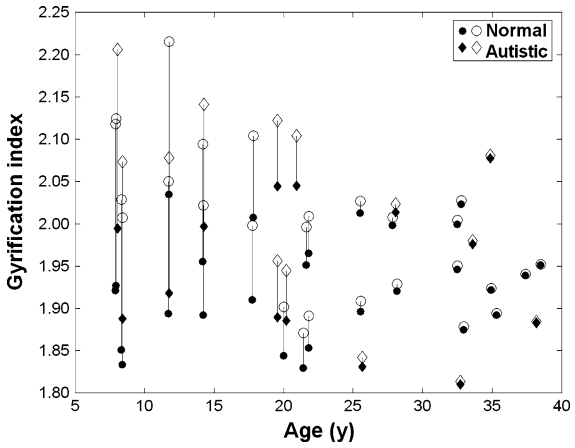

Fig. 7 Correcting GI for age. Using the model of Armstrong et al. (1995), GI measurements (*open points*) were adjusted downward to their expected value in adulthood (*filled points*) prior to statistical analysis. Following this correction, no systematic variation of GI with age is evident

Discussion

Both head circumference and structural imaging studies indicate that the brains of autistic individuals are larger than normal during the first few years of life (Courchesne et al. 2001, 2003; for cranial measurements see Dawson et al. 2007). Our neuropathological studies suggest that the basis to the described macroencephaly is an increase in the total number of minicolumns (Casanova et al. 2002a, b, 2006b). The ability of neurons to maintain connections with all other cells becomes less tenable with increasing neuronal numbers (Deacon 1990; Ringo 1991; Hofman 2001). The brain can circumvent this loss of connectivity by compartmentalizing neurons into modules. In this model, modules rather than individual cells are interconnected (Hofman 2001). Folding the cortex (increasing gyrification) decreases the distance between closely adjacent modules. This process reduces the number of interconnecting fibers, primarily long range projections, and maintains signal conduction and metabolic efficiency as brain size increases (Ringo 1991; Casanova and Tillquist 2008). Given recent studies on brain size and minicolumnar morphometry in autism, we expected that structural MRI measurements would show increased gyrification, reduced size of the corpus callosum and gray/white matter ratio, while preserving or diminishing the size of the medulla. We were also expecting that cortical thickness would be conserved or slightly widened in autistic patients (Casanova et al. 2004). In the following paragraphs we discuss the results per brain region measured and their relationship to a putative minicolumnopathy.

Gyral Window

As hypothesized, the gyral window was reduced in our autistic patients. This provides a smaller space for white matter fibers to enter or leave individual gyri and a loss of longer association fibers. This loss of fibers is supported by the observed relationship between the gyral window and the size of the corpus callosum.

The axial resistance of axoplasm to current flow varies inversely with axon diameter (Brown 2001). Bigger axonal diameters are necessary to maintain conduction velocity over longer distances. Constriction of the site of passage (reduced gyral window) of cortical afferents/efferents may limit the overall growth of wider/longer fibers, interfere with intraneuronal function, and make these fibers less efficient conveyors of signals. Neurons having these metabolically and conduction inefficient projections are weeded out during the early postnatal period (Moses et al. 2000). The resultant process is analogous to that of a compression neuropathy within the peripheral nervous system.

What could possibly cause a reduction in the gyral window in our series of autistic patients? Gross examination of postmortem brain specimens reveals no abnormalities ofgyrification (Bauman and Kemper 1985, 1994). Similarly, the neuroimaging literature portrays case reports of polymicrogyria, macrogyria, and schizencephaly as of infrequent and/or exceptional occurrence (Piven et al. 1995). Neither postmortem nor neuroimaging series lend credence to overt changes in the total number or size of gyri in the brains of autistic patients. The reduction in gyral window reported in this study may therefore reflect changes in either cortical thickness, involution of sulci, and/or complexity of gyri.

Age-related increases in cortical complexity of gyral/sulcal convolutions indicate changes in cortical topography and increased gyral branching (Blanton et al. 2001). These changes occur to a significant degree during childhood, in both hemispheres, and affect primarily the rostral (frontal) portion of the brain. Gyrification occurs following a lateral to medial gradient and coincides with rapid brain growth (Neal et al. 2007). Development of the sulcal pattern within the mesial aspect of the hemispheres (i.e., later developing gyri) is influenced by the growth of the corpus callosum (Ono et al. 1990).

Quantitative and systematic analysis of gyri in autism reveals a subtle but consistent pattern wherein sulci are shifted by 5–6 mm anteriorly and/or dorsally (Levitt et al. 2003). The re-patterning of cortical folds affects primarily the superior and inferior frontal sulci with less significant changes observed in the intraparietal and collateral sulci. Cortical folding abnormalities have also been reported using distance maps to define the white matter in cortical

gyri of autistic patients (Casanova et al. 2006a; Nordahl et al. 2007). The present study corroborates these findings using an independent population and relates the same to a bias in corticocortical connectivity.

Corpus Callosum

An argument in favor of the columnar organization of the cortex, and opposed to the single neuron model, is that there are simply not enough myelinated bundles to connect every neuron reciprocally in each hemisphere (Cook 1984). Estimates of the number of commissural fibers traversing the corpus callosum range from 200 to 500 million compared to the billions of neurons within the cerebral cortex (Cook 1984; Houzel and Milleret 1999). It may be that minicolumns and not individual neurons send and receive myelinated fibers to and from homologues in the opposite hemisphere (Cook 1984). In a study of the visual cortex of cats, Houzel and Milelret (1999) found only a minority of callosal axons performing a strict point-to-point mapping of retinotopically corresponding sites. Many of the terminals have widespread arbors demonstrating that a single callosal fiber can influence several cortical columns in the opposite hemisphere. Development of callosal axons in cat visual cortex (areas 17 and 18) reveals that from the earliest stages they grow into the gray matter in columnar like bundles. Boutons are distributed in radial columns whose diameter increases with age (Aggoun-Zouaoui et al. 1996).

The finding of a reduction in the size of the corpus callosum in the brains of autistic patients, in conjunction with the finding of smaller (and potentially more) minicolumns in autism, suggests that there is more divergence of callosal information between hemispheres. In other words, if the brains of patients with autism have smaller minicolumns while the number of callosal fibers diminishes, then the remaining/existing callosal terminals should contact more minicolumns. Houzel and Milelret (1999) postulate that the ability of callosal axons from a single area or column in one hemisphere to terminate on, and thus co-activate, multiple target neurons in several columns of the opposite hemisphere provides a potential mechanism for the grouping of individual neurons or columns into a variety of functionally coherent assemblies. This is similar to the scenario reported by Seldon (1981) whereas thalamic input to both hemispheres was similar; however, more minicolumns in the right hemisphere were contacted by thalamic terminals than were those in the left hemisphere because of the former minicolumns' proximity to each other.

Gyrification Index

The gyrification index is a ratio between the superficially exposed cortical contour and the total cortical contour, including that buried in sulci. As GI does not attempt to measure surface area, it is an unbiased measure of the degree of folding. In the course of development in utero and postnatal life, GI rises from 1, the value for a lissencephalic cortex, to a maximum value of about 3 before dropping gradually to mean adult levels of around 2.6 (Armstrong et al. 1995). The human developmental pattern is for GI to increase exponentially beginning around gestational week 25, when the brain weighs a little over 100 g, until 2.5 months postnatally, when the brain weighs approximately 600 g. Exponential growth slows until the GI peaks at 1 year of age. The GI stabilizes by 30 years of age. The time of the exponential growth of GI coincides with the time when cortico-cortical connections are being formed (Sidman and Rakic 1982). The human brain will typically more than double in mass in the following period (2.5 month–30 year). Because adult human and nonhuman anthropoid brains scale similarly with brain weight, it is likely that the maturational features which are responsible for the onset of GI development are the same for all anthropoids.

A previous MRI study of autism assessed gyrification in a single coronal slice from 30 patients with autism and 32 controls (Hardan et al. 2004). GI was higher in children with autism and adolescents, but not in adults. The authors also found that cortical folding decreased with age in patients with autism but not in controls. Despite the many merits of the study the validity of the results is hard to determine. Matching a single slice through the prefrontal cortex is difficult. Furthermore, comparative anatomical studies have shown the need for multiple measurements (a minimum of 40) within single whole brain specimens in order to provide a valid measure of gyrification (Armstrong et al. 1991).

Our findings indicated that, when correcting for brain size, there was no significant difference in the gyrification index of autistic patients and controls. The magnitude of the gyrification indices reported for all participating subjects were concordant with literature values (Casanova et al. 2004). However, the technique employed in the present study was abstracted from postmortem studies that used 2D coordinates to stack serial images (Zilles et al. 1988), thus calling into question the sensitivity of the semiautomated method. Data from the literature indicate significant discrepancies when analyzing sulcal and gyral features of cortical complexity in 2D vs. 3D (Luders et al. 2006). More sophisticated measures of cortical folding, e.g., 3D mesh-based technique, are preferred as they provide increased sensitivity and regionally specific information.

Cortical Thickness

It was hypothesized that the supernumerary minicolumns reported in autism would provide for little or no increase in cortical thickness. The results of the present study agree

with this hypothesis (see also Hutsler et al. 2007). However, we expect other experimental designs, e.g., using stochastic geometry or partitioning of gyral and sulcal gray matter, to provide for a modest increase in cortical thickness in autism (Hardan et al. 2006). Our method, which did not differentiate gray matter in sulci from that in gyri (Ferrer et al. 1988), may have diluted any findings accrued to changes in either of these compartments.

Numerous studies have shown that increases in brain size among mammals vary by more than five orders of magnitude. In contrast, cortical thickness among the same mammals varies by less than one order of magnitude (Hofman 1989; Allman 1990; Welker 1990). According to the radial-unit hypothesis of cortical development, neocortical expansion results from changes in the number of radial units (minicolumns) without a concomitant alteration in the number of neurons within each unit (Rakic 1988, 1995).

Analysis of inter- and intracluster distances of a Delaunay triangulation in autism indicates that the total number of neurons within each minicolumn is normal (Casanova et al. 2006b, c). The absence of abnormalities in cortical thickness and number of neurons per minicolumn argue against autism being the result of a dysplastic process or a disturbance of cellular migration (Piven et al. 1995; Bailey et al. 1998). The defect antedates the migration of neuroblasts and corresponds to the time when periventricular germinal cells divide symmetrically ($E < 40$) to define both the total number of minicolumns and a protomap of the cortex (Chambers and Fishell 2006).

Gray/White Matter Ratio

It has been suggested that as brain size increases, the number of interneuronal connections must decrease (Deacon 1990; Ringo 1991). This is because the cost of increased wiring and axonal length required to keep neurons at a fixed number of interconnections would be great. Organizing cells into functional units is one way to respond to having individual cells interconnected. An increase in the number of minicolumns (rather than neurons) results in increased connectivity between adjacent and more distant columns, providing a basis for increased white matter. A recent study by Herbert and associates (2004) suggests that, in autism, white matter alterations are confined to the outer (radiate) white matter compartment. This is the same compartment that provides for short range associational fibers and which is predicted to be increased given the possibility of supernumerary minicolumns (Casanova 2004). In our study, measures containing both outer and inner white matter compartments may have diluted any significant alterations that resulted from an increase in U-fiber connectivity.

Medulla

Results from our study showed reduced size of the medulla of autistic individuals as compared to controls. The medulla has been used as a control to gauge increases in neocortical volume between different mammalian species because it is considered neutral in regards to mediating intelligence (Gibson et al. 2001). The medulla may also serve as an estimator of body weight rather than encephalization (Hofman 1982). In effect, the size of the foramen magnum (medulla-spinal cord junction) has been used to control for body size differences among different species (Radinsky 1967). Using data from comparative anatomy, Deacon (1988) calculated the size of the medulla as smaller than expected for the encephalization trend observed in primates. Our results corroborate previous findings in autism of smaller than normal medulla oblongata (Hashimoto et al. 1993). These findings appear independent of development quotient or IQ (Hashimoto et al. 1992a, b). Our findings are consistent with an overall decrease in long projection fibers (corticospinal) fibers. A reduction in these fibers may help explain the motor coordination and motor skill development disorders often observed in children with autism (Baranek et al. 2005).

Functional Implications

Increased brain size and gyrification are concurrent features of encephalization. However, diverging changes in various components of brain structure argue against the human brain being a scaled-up version of the ape brain. Increases in brain volume are usually attributable to the neocortex at the expense of other components. Ringo (1991) has noted the impossibility of maintaining the same "percent connectedness" with increasing numbers of gray matter neurons. This is primarily due to the loss of longer corticocortical connections, e.g., commissural pathways. In effect, during encephalization cerebral white matter increases faster than gray matter while cross sectional measurements of the corpus callosum area fall behind those for overall brain size (Rilling and Insel 1999; Olivares et al. 2000). The consequent disconnection between otherwise homologous hemispheric areas may be responsible for the emergence of cerebral dominance. This conclusion is supported by neuroimaging studies reporting a negative correlation between language lateralization and callosal size (Hines et al. 1992). The findings imply that when information processing takes place predominantly in one hemisphere there is less need for interhemispheric information exchange. Larger brains do not increase the size of their neuronal axons to get information across longer distances. Instead, they "only connect those parts of the brain that have to be connected, and avoid the need for communication between hemispheres by

making different sides of the brain do different things" (Kaas 2004, quoted in Bradbury 2005).

Recent studies suggest that the brains of autistic patients have an increased number of minicolumns (Casanova et al. 2002a, b, 2006b). Supernumerary minicolumns have been hypothesized to provide for encephalization (Rakic 1995). During encephalization a reduced gyral window constrains the total number of afferent and efferent cortical passage fibers. Within primates decreased interhemispheric connectivity is seen as the corpus callosum becomes smaller with increasing isocortex size (Rilling and Insel 1999; Olivares et al. 2000). It may be that, as in encephalization, the increased number of minicolumns in the brains of autistic patients follows the same trend towards reducing long range connectivity. Numerous structural studies in autism have shown a reduction in the cross sectional area of the corpus callosum and/or its various subdivisions (Lainhart et al. 2005). The presence of microglia within the gray/white matter junction of autistic patients may bear witness to retractive events of long corticocortical projections as they emerge from the cortex (Vargas et al. 2005).

In autism, there is an age dependent increase in brain size which appears maximal during the first year of life (Dawson et al. 2007). Studies of brain size in adolescents and adults autistic patients are normal (Aylward et al. 2002). It thus appears that the increased number of minicolumns and neurons in the brains of autistic individuals undergo the normal maturation process of increasing the size of their cell somata, myelinating their axons, and increasing the number and complexity of synapses and dendrites. This process manifests itself as exuberant brain growth early in life only to be followed by the loss of those less efficient connections (long association fibers) that are constrained by the reduced aperture of the gyral window. These retractive events fall within a spectrum spanning normal individuals and autistic patients. Early and less severe corticocallosal lesions, contrary to those acquired after maturation, provide the possibility of fiber reorganization and acquisition of novel characteristics.

It is during the perinatal period that the different subregions of the corpus callosum are sculpted by selective elimination (Innocenti 1986; Shang et al. 1997) and lengthened in proportion to corresponding sites of cortical development (Moses et al. 2000). Abnormal postnatal retractive events happening during the maturation of the corpus callosum and other long cortico-cortical projections could account for the natural history of some autistic patients that manifest normal development followed by loss of skills and onset of symptomatology. Experience with hemispherectomies suggests that this time frame may be dictated within the first 4 years of life. During this period of time the hemispheres are equipotential with regards to linguistic abilities and a postnatal reorganization of its long corticocortical projections establishes cerebral dominance (Mariotti et al. 1998; Devlin et al. 2003). This inherent neuroplasticity is not a property of the abnormal brain (e.g., those with hemispherectomies); but rather, a re-organizing mechanism propelled by epigenetic influences that appears most salient at defined periods of brain development and aging (Doidge 2007).

Acknowledgments The series of patients and controls were collected under the guidance and support of Dr. Judith Rapoport, Chief of the Child Psychiatry Branch at the National institute of Mental Heath.

References

Adalsteinsson, D., & Sethian, J. A. (1995). A fast level set method for propagating interfaces. *Journal of Computational Physics, 118*, 269–277. doi:10.1006/jcph.1995.1098.

Aggoun-Zouaoui, D., Kiper, D. C., & Innocenti, G. M. (1996). Growth of callosal terminal arbors in primary visual areas of the cat. *The European Journal of Neuroscience, 8*, 1132–1148. doi:10.1111/j.1460-9568.1996.tb01281.x.

Allman, J. M. (1990). Evolution of neocortex. In E. G. Jones & A. Peters (Eds.), *Comparative structure and evolution of cerebral cortex* (pp. 269–283). New York: Plenum Press.

Armstrong, E., Curtis, M., Fregoe, C., Zilles, K., Casanova, M. F., & McCarthy, W. (1991). Cortical gyrification in the rhesus monkey: A test of the mechanical folding hypothesis. *Cerebral Cortex (New York, N.Y.), 1*, 426–432. doi:10.1093/cercor/1.5.426.

Armstrong, E., Schleicher, A., Omran, H., Curtis, M., & Zilles, K. (1995). The ontogeny of human gyrification. *Cerebral Cortex (New York, N.Y.), 5*, 56–63. doi:10.1093/cercor/5.1.56.

Aylward, E. H., Minshew, N. J., Field, K., Sparks, B. F., & Singh, N. (2002). Effects of age on brain volume and head circumference in autism. *Neurology, 59*, 158–159.

Bailey, A., Luthert, P., Dean, A., Harding, B., Janota, I., Montgomery, M., et al. (1998). A clinicopathological study of autism. *Brain, 121*, 889–905. doi:10.1093/brain/121.5.889.

Bailey, A., Phillips, W., & Rutter, M. (1996). Autism: Toward an integration of clinical, genetic, neuropsychological, and neurobiological perspectives. *Journal of Child Psychology and Psychiatry and Allied Disciplines, 37*, 39–126. doi:10.1111/j.1469-7610.1996.tb01381.x.

Baranek, G. T., Parham, D., & Bodfish, J. W. (2005). Sensory and motor features in autism: Assessment and intervention. In F. R. Volkmar, R. Paul, A. Lin, & D. Cohen (Eds.), *Handbook of autism and pervasive developmental disorders, vol. 2: Assessment, interventions, and policy* (pp. 831–857). New Jersey: Wiley.

Bauman, M. L., & Kemper, T. L. (1985). Histoanatomic observations of the brain in early infantile autism. *Neurology, 35*, 866–874.

Bauman, M. L., & Kemper, T. L. (1988). Limbic and cerebellar abnormalities: Consistent findings in infantile autism. *Journal of Neuropathology and Experimental Neurology, 47*, 369.

Bauman, M. L., & Kemper, T. L. (1994). Neuroanatomic observations of the brain in autism. In M. L. Bauman & T. L. Kemper (Eds.), *The neurobiology of autism* (pp. 119–145). Baltimore: The Johns Hopkins University Press.

Blanton, R. E., Levitt, J. G., Thompson, P. M., Narr, K. L., Capetillo-Cunliffe, L., Nobel, A., et al. (2001). Mapping cortical asymmetry and complexity patterns in normal children. *Psychiatry Research: Neuroimaging, 107*, 29–43. doi:10.1016/S0925-4927(01)00091-9.

Bouman, C., & Sauer, K. (1993). A generalized Gaussian image model for edge-preserving MAP estimation. *IEEE Transactions on Image Processing, 2*, 296–310. doi:10.1109/83.236536.

Bradbury, J. (2005). Molecular insights into human brain evolution. *PLoS Biology, 3*, e50. doi:10.1371/journal.pbio.0030050.

Brodmann, K. (1913). Neue Forschungsergebnisse der Grosshirnrindenanatomie mit besonderer Berücksichtigung anthropologischer Fragen. *Verhandlungen der Gesellschaft Deutscher Naturforscher und Ärzte, 85*, 200–240.

Brown, A. G. (2001). *Nerve cells and nervous systems: An introduction to neuroscience* (2nd ed.). London: Springer.

Buxhoeveden, D. P., Semendeferi, K., Buckwalter, J., Schenker, N., Switzer, R., & Courchesne, E. (2006). Reduced minicolumns in the frontal cortex of patients with autism. *Neuropathology and Applied Neurobiology, 32*, 483–491. doi:10.1111/j.1365-2990.2006.00745.x.

Casanova, M. F. (2004). White matter volume increase and minicolumns in autism. *Annals of Neurology, 56*, 453. doi:10.1002/ana.20196.

Casanova, M. F., Araque, J., Giedd, J., & Rumsey, J. M. (2004). Reduced brain size and gyrification in the brains of dyslexic patients. *Journal of Child Neurology, 19*, 275–281. doi:10.1177/088307380401900407.

Casanova, M. F., Buxhoeveden, D., Switala, A., & Roy, E. (2002a). Minicolumnar pathology in autism. *Neurology, 58*, 428–432.

Casanova, M. F., Buxhoeveden, D., Switala, A., & Roy, E. (2002b). Neuronal density and architecture (gray level index) in the brains of autistic patients. *Journal of Child Neurology, 17*, 515–521. doi:10.1177/088307380201700708.

Casanova, M. F., Farag, A., El-Baz, A., Mott, M., Hassan, H., Fahmi, R., Switala, A. E. (2006a). Abnormalities of the gyral window in autism: A macroscopic correlate to a putative minicolumnopathy. *Journal of Special Education and Rehabilitation, 1*(1–2), 85–101.

Casanova, M. F., & Tillquist, C. (2008). Encephalization, emergent properties, and psychiatry: A minicolumnar perspective. *The Neuroscientist, 14*, 101–118. doi:10.1177/1073858407309091.

Casanova, M. F., Van Kooten, I. A. J., Switala, A. E., Van Engeland, H., Heinsen, H., Steinbusch, H. W. M., et al. (2006b). Minicolumnar abnormalities in autism. *Acta Neuropathologica, 112*, 287–303. doi:10.1007/s00401-006-0085-5.

Casanova, M. F., Van Kooten, I., Switala, A. E., Van England, H., Heinsen, H., Steinbuch, H. W. M., et al. (2006c). Abnormalities of cortical minicolumnar organization in the prefrontal lobes of autistic patients. *Clinical Neuroscience Research, 6*, 127–133. doi:10.1016/j.cnr.2006.06.003.

Chambers, D., & Fishell, G. (2006). Functional genomics of early cortex patterning. *Genome Biology, 7*, 202. doi:10.1186/gb-2006-7-1-202.

Chenn, A., & Walsh, C. A. (2003). Increased neuronal production, enlarged forebrains, and cytoarchitectural distortions in β-catenin overexpressing transgenic mice. *Cerebral Cortex (New York, N.Y.), 13*, 599–606. doi:10.1093/cercor/13.6.599.

Cook, N. D. (1984). Homotopic callosal inhibition. *Brain and Language, 23*, 116–125. doi:10.1016/0093-934X(84)90010-5.

Courchesne, E., Carper, R. A., & Akshoomoff, N. A. (2003). Evidence of brain overgrowth in the first year of life in autism. *Journal of the American Medical Association, 290*, 337–344. doi:10.1001/jama.290.3.337.

Courchesne, E., Karns, C. M., Davis, H. R., Ziccardi, R., Carper, R. A., Tigue, Z. D., et al. (2001). Unusual brain growth patterns in early life in patients with autistic disorder: An MRI study. *Neurology, 57*, 245–254.

Courchesne, E., Muller, R. A., & Saitoh, O. (1999). Brain weight in autism: Normal in the majority of cases, megaloencephalic in rare cases. *Neurology, 52*, 1057–1059.

Dawson, G., Munson, J., Webb, S. J., Nalty, T., Abbott, R., & Toth, K. (2007). Rate of head growth decelerates and symptoms worsen in the second year of life in autism. *Biological Psychiatry, 61*, 458–464. doi:10.1016/j.biopsych.2006.07.016.

Deacon, T. W. (1988). Human brain evolution, II: Embryology and brain allometry. In H. Jerison & I. Jerison (Eds.), *Intelligence and evolutionary biology* (pp. 383–415). Berlin: Springer.

Deacon, T. W. (1990). Rethinking mammalian brain evolution. *American Zoologist, 30*, 629–705.

Devlin, A. M., Cross, J. H., Harkness, W., Chong, W. K., Harding, B., Vargha-Khadem, F., et al. (2003). Clinical outcomes of hemispherectomy for epilepsy in childhood and adolescence. *Brain, 126*, 556–566. doi:10.1093/brain/awg052.

Doidge, N. (2007). *The brain that changes itself*. New York: Viking.

El-Baz, A., Casanova, M. F., Gimel'farb, G., Mott, M., & Switala, A. E. (2007a). A new image analysis approach for automatic classification of autistic brains. In *IEEE Engineering in Medicine and Biology Society, Biomedical imaging: Macro to nano* (pp. 352–355). Piscataway, NJ: IEEE.

El-Baz, A., Casanova, M. F., Gimel'farb, G., Mott, M., & Switala, A. (2007b). Autism diagnostics by 3D texture analysis of cerebral white matter gyrifications. In N. Ayache, S. Ourselin, & A. Maeder (Eds.), *Medical image computing and computer-assisted intervention—MICCAI 2007 (part II)* (pp. 882–890). New York: Springer.

El-Baz, A., Farag, A., Ali, A., Gimel'farb, G., & Casanova, M. (2006). A framework for unsupervised segmentation of multimodal medical images. In R. R. Beichel & M. Sonka (Eds.), *Computer vision approaches to medical image analysis* (pp. 120–131). New York: Springer.

Fahmi, R., Aly, A., El-Baz, A., & Farag, A. A. (2006). New deformable registration technique using scale space and curve evolution theory and a finite element based validation framework. *Proceedings of the Annual International Conference of the IEEE Engineering in Medicine and Biology Society, 28*, 3041–3044.

Fahmi, R., El-Baz, A., Hassan, H., Farag, A., & Casanova, M. F. (2007). Classification techniques for autistic vs. typically developing brain using MRI data. In *Biomedical imaging: From nano to macro* (pp. 1348–1351). Piscataway, NJ: IEEE.

Ferrer, I., Hernández-Martí, M., Bernet, E., & Galofré, E. (1988). Formation and growth of the cerebral convolutions, I: Postnatal development of the median-suprasylvian gyrus and adjoining sulci in the cat. *Journal of Anatomy, 160*, 89–100.

Friede, R. L. (1989). *Developmental neuropathology* (2nd ed.). Berlin: Springer.

Gibson, K. R., Rumbaugh, D., & Beran, M. (2001). Bigger is better: Primate brain size in relationship to cognition. In D. Falk & K. R. Gibson (Eds.), *Evolutionary anatomy of the primate cerebral cortex* (pp. 79–97). Cambridge: Cambridge University Press.

Goldberg, J., Szatmari, P., & Nahmias, C. (1999). Imaging of autism: Lessons from the past to guide studies in the future. *Canadian Journal of Psychiatry, 44*, 793–801.

Hardan, A. Y., Jou, R. J., Keshavan, M. S., Varma, R., & Minshew, N. J. (2004). Increased frontal cortical folding in autism: A preliminary MRI study. *Psychiatry Research, 131*, 263–268. doi:10.1016/j.pscychresns.2004.06.001.

Hardan, A. Y., Muddasani, S., Vemulapalli, M., Keshevan, M. S., & Minshew, N. J. (2006). An MRI study of increased cortical thickness in autism. *The American Journal of Psychiatry, 163*, 1290–1292. doi:10.1176/appi.ajp.163.7.1290.

Hashimoto, T., Murakawa, K., Miyazaki, M., Tayama, M., & Kuroda, Y. (1992a). Magnetic resonance imaging of the brain structures in the posterior fossa in retarded autistic children. *Acta Paediatrica (Oslo, Norway), 81*, 1030–1034. doi:10.1111/j.1651-2227.1992.tb12169.x.

Hashimoto, T., Tayama, M., Miyazaki, M., Murakawa, K., Shimakawa, S., Yoneda, Y., et al. (1993). Brainstem involvement in high-functioning autistic children. *Acta Neurologica Scandinavica, 88*, 123–128.

Hashimoto, T., Tayama, M., Miyazaki, M., Sakurama, N., Yoshimoto, T., Murakawa, K., et al. (1992b). Reduced brainstem size in children with autism. *Brain and Development, 14*, 94–97.

Haydar, T. F., Bambrick, L. L., Krueger, B. K., & Rakic, P. (1999). Organotypic slice cultures for analysis of proliferation, cell death, and migration in the embryonic neocortex. *Brain Research Protocols, 4*, 425–437. doi:10.1016/S1385-299X(99)00033-1.

Herbert, M. R. (2005). Large brains in autism: The challenge of pervasive abnormalities. *The Neuroscientist, 11*, 417–440. doi:10.1177/0091270005278866.

Herbert, M. R., Ziegler, D. A., Makris, N., Filipek, P. A., Kemper, T. L., Normandin, J. J., et al. (2004). Localization of white matter volume increase in autism and developmental language disorder. *Annals of Neurology, 55*, 530–540. doi:10.1002/ana.20032.

Hines, M., Chiu, I., McAdams, L. A., Bentler, P. M., & Lipcamon, J. (1992). Cognition and the corpus callosum: Verbal fluency, visuospatial ability, and language lateralization related to midsagittal surface areas of callosal subregions. *Behavioral Neuroscience, 106*, 3–14. doi:10.1037/0735-7044.106.1.3.

Hofman, M. A. (1982). Encephalization in mammals in relation to the size of the cerebral cortex. *Brain, Behavior and Evolution, 20*, 84–96. doi:10.1159/000121583.

Hofman, M. A. (1989). On the evolution and geometry of the brain in mammals. *Progress in Neurobiology, 32*, 137–158. doi:10.1016/0301-0082(89)90013-0.

Hofman, M. A. (2001). Brain evolution in hominids: Are we at the end of the road? In D. Falk & K. R. Gibson (Eds.), *Evolutionary anatomy of the primate cerebral cortex* (pp. 113–127). Cambridge: Cambridge University Press.

Houzel, J. C., & Milleret, C. (1999). Visual inter-hemispheric processing: Constraints and potentialities set by axonal morphology. *Journal de Physiologie, 93*, 271–284.

Hutsler, J. J., Love, T., & Zhang, H. (2007). Histological and magneticresonance imaging assessment of cortical layering and thickness in autism spectrum disorders. *Biological Psychiatry, 61*, 449–457. doi:10.1016/j.biopsych.2006.01.015.

Innocenti, G. M. (1986). General organization of callosal connections in the cerebral cortex. In E. G. Jones (Ed.), *Cerebral cortex, vol. 5: Sensory-motor area and aspects of cortical connectivity* (pp. 291–353). New York: Springer.

Kaas, J. H. (2004). Evolution of somatosensory and motor cortex in primates. *The Anatomical Record, 281A*, 1148–1156. doi:10.1002/ar.a.20120.

Kass, M., Witkin, A., & Terzopoulos, D. (1988). Snakes: Active contour models. *International Journal of Computer Vision, 1*, 321–331. doi:10.1007/BF00133570.

Keller, T. A., Kana, R. K., & Just, M. A. (2007). A developmental study of the structural integrity of white matter in autism. *NeuroReport, 18*, 23–27. doi:10.1097/01.wnr.0000239965.21685.99.

Kuida, K., Zheng, T. S., Na, S., Kuang, C. Y., Yang, D., Karasuyama, H., et al. (1996). Decreased apoptosis in the brain and premature lethality in CPP32-deficient mice. *Nature, 384*, 368–372. doi:10.1038/384368a0.

Lainhart, J. E., Lazar, M., Bigler, E. D., & Alexander, A. (2005). The brain during life in autism: Advances in neuroimaging research. In M. F. Casanova (Ed.), *Recent developments in autism research* (pp. 57–108). New York: Nova Biomedical.

Levitt, J. G., Blanton, R. E., Smalley, S., Thompson, P. M., Guthrie, D., McCracken, J. T., et al. (2003). Cortical sulcal maps in autism. *Cerebral Cortex (New York, N.Y.), 13*, 728–735. doi:10.1093/cercor/13.7.728.

Luders, E., Thompson, P. M., Narr, K. L., Toga, A. W., Lancke, L., & Gaser, C. (2006). A curvature-based approach to estimate local gyrification on the cortical surface. *NeuroImage, 29*, 1224–1230. doi:10.1016/j.neuroimage.2005.08.049.

Mariotti, P., Iuvone, L., Torrioli, M. G., & Silveri, M. C. (1998). Linguistic and non-linguistic abilities in a patient with early left hemispherectomy. *Neuropsychologia, 36*, 1303–1312. doi:10.1016/S0028-3932(98)00031-1.

Moses, P., Courchesne, E., Stiles, J., Trauner, D., Egaas, B., & Edwards, E. (2000). Regional size reduction in the human corpus callosum following pre- and perinatal brain injury. *Cerebral Cortex (New York, N.Y.), 10*, 1200–1210. doi:10.1093/cercor/10.12.1200.

Neal, J., Takahashi, M., Silva, M., Tiao, G., Walsh, C. A., & Sheen, V. L. (2007). Insights into the gyrification of developing ferret brain by magnetic resonance imaging. *Journal of Anatomy, 210*, 66–77. doi:10.1111/j.1469-7580.2006.00674.x.

Nordahl, C. W., Dierker, D., Mostafavi, I., Schumann, C. M., Rivera, S. M., Amaral, D. G., et al. (2007). Cortical folding abnormalities in autism revealed by surface-based morphometry. *The Journal of Neuroscience, 27*, 11725–11735. doi:10.1523/JNEUROSCI.0777-07.2007.

Olivares, R., Michalland, S., & Aboitiz, F. (2000). Cross-species and intraspecies morphometric analysis of the corpus callosum. *Brain, Behavior and Evolution, 55*, 37–43. doi:10.1159/000006640.

Ono, M., Kubik, S., & Abernathey, C. D. (1990). *Atlas of cerebral sulci*. New York: Thieme.

Piven, J., Arndt, S., Bailey, J., & Andreasen, N. (1996). Regional brain enlargement in autism: A magnetic resonance imaging study. *Journal of the American Academy of Child and Adolescent Psychiatry, 35*, 530–536.

Piven, J., Arndt, S., Bailey, J., Havercamp, S., Andreason, N. C., & Palmer, P. (1995). An MRI study of brain size in autism. *The American Journal of Psychiatry, 152*, 1145–1149.

Prothero, J. W., & Sundsten, J. W. (1984). Folding of the cerebral cortex in mammals: A scaling model. *Brain, Behavior and Evolution, 24*, 152–167. doi:10.1159/000121313.

Radinsky, L. (1967). Relative brain size: A new measure. *Science, 155*, 836–838. doi:10.1126/science.155.3764.836.

Rakic, P. (1988). The specification of cerebral cortical areas: The radial unit hypothesis. *Science, 241*, 928–931. doi:10.1126/science.3291116.

Rakic, P. (1995). One small step for the cell, a giant leap for mankind: A hypothesis of neocortical expansion during evolution. *Trends in Neurosciences, 18*, 383–388. doi:10.1016/0166-2236(95)93934-P.

Rilling, J. K., & Insel, T. R. (1999). The primate neocortex in comparative perspective using magnetic resonance imaging. *Journal of Human Evolution, 37*, 191–223. doi:10.1006/jhev.1999.0313.

Ringo, J. L. (1991). Neuronal interconnection as a function of brain size. *Brain, Behavior and Evolution, 38*, 1–6. doi:10.1159/000114375.

Seldon, H. L. (1981). Structure of human auditory cortex, II: Axon distributions and morphological correlates of speech perception. *Brain Research, 229*, 295–310. doi:10.1016/0006-8993(81)90995-1.

Shang, F., Ashwell, K. W. S., Marotte, L. R., & Waite, P. M. E. (1997). Development of commisural neurons in the wallaby (*Macropus eugenii*). *The Journal of Comparative Neurology, 387*, 507–523. doi:10.1002/(SICI)1096-9861(19971103)387:4<507::AID-CNE3>3.0.CO;2-6.

Sidman, R. L., & Rakic, P. (1982). Development of the human central nervous system. In W. Haymaker & A. D. Adams (Eds.), *Histology and histopathology of the nervous system* (pp. 3–145). Springfield, Ill: Charles C. Thomas.

Sparks, B. F., Friedman, S. D., Shaw, D. W., Aylward, E. H., Echelard, D., Artru, A. A., et al. (2002). Brain structural

abnormalities in young children with autism spectrum disorder. *Neurology, 59*, 158–159.

Szatmari, P., Bremner, R., & Nagy, J. (1989). Asperger's syndrome: A review of clinical features. *Canadian Journal of Psychiatry, 34*, 554–560.

Tarui, T., Takahashi, T., Nowakowski, R. S., Hayes, N. L., Bhide, P. G., & Caviness, V. S. (2005). Overexpression of $p27^{Kip1}$, probability of cell cycle exit, and laminar destination of neocortical neurons. *Cerebral Cortex (New York, N.Y.), 15*, 1343–1355. doi:10.1093/cercor/bhi017.

Vargas, D., Nascimbene, C., Krishnan, C., Zimmerman, A., & Pardo, C. (2005). Neuroglial activation and neuroinflammation in the brain of patients with autism. *Annals of Neurology, 57*, 67–81. doi:10.1002/ana.20315.

Welker, W. (1990). Why does cerebral cortex fissure and fold? A review of determinants of gyri and sulci. In E. G. Jones & A. Peters (Eds.), *Comparative structure and evolution of cerebral cortex* (pp. 3–136). New York: Plenum Press.

Zilles, K., Armstrong, E., Moser, K. H., & Schleicher, A. (1989). Gyrification in the cerebral cortex of primates. *Brain, Behavior and Evolution, 34*(3), 143–150. doi:10.1159/000116500.

Zilles, K., Armstrong, E., Schleicher, A., & Kretschmann, H. J. (1988). The human pattern of gyrification in the cerebral cortex. *Anatomy and Embryology, 179*, 173–179. doi:10.1007/BF00304699.